

# A general approach to advective–dispersive transport with multirate mass transfer

P. Patrick Wang<sup>a</sup>, Chunmiao Zheng<sup>b,\*</sup>, Steven M. Gorelick<sup>c</sup>

<sup>a</sup> Department of Mathematics, University of Alabama, Tuscaloosa, AL 35487, USA

<sup>b</sup> Department of Geological Sciences, University of Alabama, Tuscaloosa, AL 35487, USA

<sup>c</sup> Department of Earth & Environmental Sciences, Stanford University, Stanford, CA 94305, USA

Received 31 December 2003; received in revised form 27 September 2004; accepted 4 October 2004

## Abstract

A numerical solution that is significantly more general than other semi-analytical solutions is presented for governing equations describing advective–dispersive transport with multirate mass transfer between mobile and immobile domains. The new solution approach is general in the sense that it does not impose any restrictive assumption on the spatial or temporal variability of advective and dispersive processes in the mobile domain. A single integro-differential equation (IDE) is developed for the concentration in the mobile domain by separating the concentration in the immobile domain from the set of two partial differential equations. The solution to the IDE requires the evaluation of a temporal integral of the concentration in the mobile domain, which is a function of the Laplace transform of the distribution of the mass transfer rate coefficient. The Laplace transform is not limited to flow fields with known constant velocities. The solutions for one- and two-dimensional examples obtained using the new approach agree with those obtained by existing semi-analytical and numerical approaches.

© 2004 Elsevier Ltd. All rights reserved.

*Keywords:* Dual-domain model; Multirate mass transfer; Advective–dispersive transport; Laplace transform; Contaminant transport modeling

## 1. Introduction

Since the 1950s the dual-domain model has been used to represent physical and chemical nonequilibrium mass transfer processes controlled by diffusion that occur during solute advection and dispersion (e.g., [10,1,8,4]). The simplest nonequilibrium mass transfer between a “mobile” domain and an “immobile” domain is approximated as a first-order exchange dictated by a single rate coefficient (e.g., [28,30,25,26,20,34,3,11]). A concise review of the many different mathematical forms of the dual-domain model can be found in Haggerty and Gorelick [12]. The single-rate dual-domain model continues

to be applied successfully to field problems (e.g., [32,9,19,23]).

A far more comprehensive and generalized description of mass transfer between mobile and immobile domains is the multirate model (e.g., [31,2,29,27]). It accounts for simultaneous mass transfer processes, governed by multiple first-order equations and a set of mass transfer rate coefficients following a probability density function (e.g., [12]). The multirate model significantly extends the simple dual-domain concept to problems involving a variety of rate-limited mass-transfer processes that are likely to occur in heterogeneous media due to both diffusion and slow advection. The multirate model achieves better agreement with tracer data from both laboratory columns and field experiments than the single-rate model (e.g., [7,13,22,16,17,24]).

Analytical or numerical solutions of the advection–dispersion equation incorporating multirate mass

\* Corresponding author. Tel.: +1 205 348 0579; fax: +1 205 348 0818.

E-mail address: [czheng@ua.edu](mailto:czheng@ua.edu) (C. Zheng).

transfer are not trivial. Haggerty and Gorelick [12] used a Laplace transform to obtain an analytical solution for 1-D transport in a radial flow field. The analytical solution in the Laplace domain was inverted numerically to the time-domain. The semi-analytical approach has been implemented in computer codes [15,14] and used to analyze single-well and two-well tracer tests (e.g., [17,24]). The semi-analytical solution is limited, however, to steady-state and linear groundwater flow fields.

Culver et al. [7] proposed an approach that discretized a continuous probability density function (PDF) for a multirate model into a finite number of “compartments”, or “bins”, each of which was assumed to behave as a single-rate model. This approach is quite general and can be used in conjunction with standard finite-difference or finite-element methods to solve multidimensional advective–dispersive transport subject to multirate mass transfer [6]. However, the approach is approximate with its accuracy depending on the number and different sizes of selected compartments.

We present a new approach to the solution of multirate mass transfer coupled with advective–dispersive transport. The approach is more general than the semi-analytical approach because no steady or linear flow conditions are imposed, and it is more accurate than the compartment approach because no discretization is required for the probability density function of the mass transfer rate coefficients. Here, we provide an overview of the multirate mass transfer model, describe the proposed solution approach, and then apply it to two illustrative examples for comparison with the semi-analytical solution of Haggerty and Reeves [14] and the numerical solution obtained using the general transport simulator MT3DMS [33].

## 2. Multirate mass transfer model

The partial differential equation (PDE) that governs transport during multirate-limited mass transfer is given, for the mobile domain, as follows (e.g., [12])

$$\frac{\partial C_m}{\partial t} + \phi \int_0^\infty f(\beta) \frac{\partial C_{im}}{\partial t} d\beta = L(C_m) \quad (1)$$

where  $C_m$  and  $C_{im}$  are the solute concentrations in the mobile and immobile domains, respectively;  $\phi = \theta_{im}/\theta_m$  is the ratio of the immobile domain porosity over the mobile domain porosity;  $f(\beta)$  is a probability distribution function of the continuous set of first-order rates controlling mass transfer between mobile and immobile domains and satisfying  $\int_0^\infty f(\beta) d\beta = 1$ ;  $L(C_m)$  is the operator representing the advection and dispersion of solutes, and fluid sources/sinks in the mobile domain. The gamma and lognormal distribution functions are commonly used when parameters are strictly nonnegative. It should be pointed out that, although many

probability density functions can be used in characterizing the distribution of the mass transfer rate coefficient, the mass transfer rate coefficient is not a random variable. Rather it is a deterministic function. The terms *distribution function* and *density function* are used interchangeably. For later use, we need to define the  $n$ th moment of the distribution denoted by a bracket  $\langle \cdot \rangle$ , i.e.,  $\langle \beta^n \rangle = \int_0^\infty \beta^n f(\beta) d\beta$ .

The governing PDE for the immobile domain is given as

$$\frac{\partial C_{im}}{\partial t} = \beta(C_m - C_{im}), \quad 0 < \beta < \infty \quad (2)$$

which holds for every value of  $\beta$  so that the concentration in the immobile domain is a function of the rate coefficient  $\beta$ . Furthermore, the rate coefficient  $\beta$  as used in (2) follows the convention of Haggerty and Gorelick [12] and Harvey and Gorelick [19], which differs from the rate coefficient  $\beta^*$  used in Zheng and Wang [33] and Feehley et al. [9] by a factor of  $\theta_{im}$ , i.e.,  $\beta = \beta^*/\theta_{im}$ .

It is noteworthy that although this paper is focused on physical nonequilibrium of diffusional nature, the solution approach developed in this study is equally applicable to chemical nonequilibrium caused by linear multirate sorption (e.g., [7]). This is because the governing equations for dual-domain mass transfer, either single-rate or multirate, are mathematically identical for the two types of nonequilibrium as demonstrated in previous studies (e.g., [12,33]).

The initial conditions for mobile and immobile domains can be expressed, respectively, as

$$C_m(0) = C_m^0 \quad (3a)$$

$$C_{im}(0) = C_{im}^0 \quad (3b)$$

where  $C_m^0$  and  $C_{im}^0$  are the known initial concentrations in the mobile and immobile domains, respectively. Here the initial concentration in the mobile domain,  $C_m^0$ , is a spatial function, while the initial concentration in the immobile domain,  $C_{im}^0$ , is not only a spatial function but also has a value corresponding to each local mass transfer rate coefficient in the density function.

Multiplying both sides of (2) by  $f(\beta)$  and integrating with respect to  $\beta$  from zero to infinity yields

$$\int_0^\infty f(\beta) \frac{\partial C_{im}}{\partial t} d\beta = \int_0^\infty f(\beta) \beta (C_m - C_{im}) d\beta \quad (4)$$

The PDEs for both mobile and immobile domains can also be rewritten in standard form as

$$\frac{\partial C_m}{\partial t} = L(C_m) - \phi \int_0^\infty f(\beta) \beta (C_m - C_{im}) d\beta \quad (5a)$$

$$\frac{\partial C_{im}}{\partial t} = \beta(C_m - C_{im}), \quad 0 < \beta < \infty \quad (5b)$$

where the initial conditions are defined in (3a) and (3b).

### 3. Solution methods

#### 3.1. Basic strategy

Our approach to solving the coupled system (5) consists of two steps. The first step is to eliminate the concentration in the immobile domain from the set of two coupled PDEs and the second step is to obtain the solution. Note that the advection–dispersion term  $L(C_m)$  in (5) can be solved by any standard transport solution technique such as the finite difference method, the method of characteristics, and the total-variation-diminishing (TVD) scheme as dictated by the efficiency and accuracy constraints (see [33]).

From (2) we first solve for  $C_{im}$ , the concentration in the immobile domain, in terms of  $C_m$ . Since it is a linear, first-order differential equation, the solution can be readily obtained as

$$C_{im} = e^{-\beta t} \left[ C_{im}^0 + \int_0^t e^{\beta \tau} \beta C_m d\tau \right] \quad (6)$$

where  $\tau$  is the temporal integration variable. Substituting the above solution into (5) and exchanging the order of integration, which is permissible, lead us to

$$\begin{aligned} \frac{\partial C_m}{\partial t} &= L(C_m) - \phi \int_0^\infty \left\{ f(\beta) \beta \left[ C_m - e^{-\beta t} \right. \right. \\ &\quad \left. \left. \times \left( C_{im}^0 + \int_0^t e^{\beta \tau} \beta C_m d\tau \right) \right] \right\} d\beta \\ &= L(C_m) - \phi C_m \int_0^\infty f(\beta) \beta d\beta + \phi \int_0^\infty C_{im}^0 f(\beta) \beta e^{-\beta t} d\beta \\ &\quad + \phi \left[ \int_0^t C_m(\tau) \int_0^\infty f(\beta) \beta^2 e^{-\beta(t-\tau)} d\beta d\tau \right] \end{aligned} \quad (7)$$

There are four terms on the right-hand side of the equation; the first term is the sum of advection, dispersion and sinks/sources in the mobile domain and the other three terms are due to mass exchange between mobile and immobile domains. The mass exchange terms are all in integral form. The first integral is related to the mean value of the mass transfer rate coefficient,  $\langle \beta \rangle$ ; the second integral represents the release of the initial concentration in the immobile domain  $C_{im}^0$ . Finally, the third integral involves the higher-moments of the mass transfer rate coefficient distribution function and the history of the concentration in the mobile domain from simulation time zero to current time  $t$ .

To further simplify the above equation we define two integral functions by  $g(t)$  and  $H(t)$ , respectively, as

$$g(t) = \int_0^\infty C_{im}^0 f(\beta) \beta e^{-\beta t} d\beta \quad (8a)$$

$$H(t) = \int_0^\infty f(\beta) \beta^2 e^{-\beta t} d\beta \quad (8b)$$

Note that both functions  $g$  and  $H$  are integrals containing the same negative exponential term  $e^{-\beta t}$  with respect to mass transfer rate coefficient from zero to infinity. A variant of the  $g(t)$  function, i.e., without the term  $C_{im}^0$ , was used by Carrera et al. [5] and Haggerty et al. [16] and referred to as the “memory function”. Substituting these functions into (5) results in an integro-differential equation (IDE):

$$\frac{\partial C_m}{\partial t} = L(C_m) - \phi \langle \beta \rangle C_m + \phi g(t) + \phi \int_0^t H(t - \tau) C_m(\tau) d\tau \quad (9)$$

with the initial condition  $C_m(0) = C_m^0$ . It is noteworthy that Haggerty et al. [16,18] have also showed that the mobile–immobile mass transfer can be expressed as a sink/source term in the governing equation for the mobile domain, resulting in another form of the IDE that is somewhat simpler and has the advantage of having been studied in the mathematics literature.

Note that the term  $-\phi \langle \beta \rangle C_m$  representing the mass transferred into the immobile domain has the same form as a first-order decay term. If this term is included into the advection–dispersion operator as  $L'(C_m) = L(C_m) - \phi \langle \beta \rangle C_m$ , we can simplify (9) further as

$$\frac{\partial C_m}{\partial t} = L'(C_m) + \phi g(t) + \phi \int_0^t H(t - \tau) C_m(\tau) d\tau \quad (10)$$

The resulting IDE (10) involves two time-dependent functions,  $g$  and  $H$ , that have to be determined before the solution to the IDE can be obtained. We will show next that those two functions are related to the Laplace transform (LT) of the mass transfer rate coefficient density function. Additional information is given in Appendix A on the evaluation of the  $g$  and  $H$  functions if the LT is not available for certain distribution functions.

The LT of a function, say  $f(t)$  for a nonnegative variable  $t$ , is an integral transformation from one domain (usually the time domain) into another domain (usually the frequency domain)

$$\overline{f(s)} = \int_0^\infty e^{-st} f(t) dt \quad (11)$$

provided that the integral exists. LT techniques have been used extensively to solve linear differential equations. One of the advantages of LT is that it changes differential equations into algebraic equations, which are much simpler to solve. Inverting the LT will give the desired solution in the time domain. The major limitation, however, is that it assumes linear differential equations and time-invariant coefficients. In subsequent discussions, we will demonstrate that our approach is applicable to solving general transport equations with multirate mass transfer under spatially and temporally variable velocity distributions.

Inspection of (8) and comparison with the definition of the LT in (11) reveal that both functions  $g(t)$  and  $H(t)$  are closely related to Laplace transforms. If we denote by  $\overline{f(s)}$  the LT for  $f(\beta)$ ,

$$\overline{f(s)} = \int_0^\infty e^{-s\beta} f(\beta) d\beta \quad (12)$$

and we differentiate the above LT function twice with respect to Laplace variable  $s$  and then replace it by time,  $t$ , an immediate result is

$$H(t) = \left. \frac{d^2 \overline{f(s)}}{ds^2} \right|_{s=t} \quad (13)$$

The relation (13) deserves some comments regarding two important features exploited in our approach that create significant generality. First, (13) enables us to use the LT of the mass transfer rate coefficient. This is because of the fact that after the transformation, the distribution function, which has infinite dimension, disappears. The Laplace variable happens to be the time  $t$ , so that we do not have to introduce the additional Laplace variable and more importantly, we do not need to invert the LT. Inversion of the LT is often done numerically, which can be a difficult task and is subject to numerical errors. Second, because this LT is about the density function, we need not assume linearity of the PDE under consideration, nor require time-invariance of the coefficients involved in the PDE. Our rate-based transform approach enables us to handle nonuniform and time-varying velocities and dispersion coefficients.

Now consider the other function,  $g(t)$ . If the initial concentration in the immobile domain,  $C_{im}^0$ , does not depend on the value of the mass transfer rate coefficient  $\beta$  (which may vary spatially), we can move  $C_{im}^0$  out of the integral to yield

$$g(t) = C_{im}^0 \int_0^\infty f(\beta) \beta e^{-\beta t} d\beta \quad (14)$$

The integral is equivalent to the derivative of the LT evaluated at  $t$

$$g(t) = -C_{im}^0 \left. \frac{d\overline{f(s)}}{ds} \right|_{s=t} \quad (15)$$

In case the initial concentration  $C_{im}^0$  varies with transfer rate coefficient  $\beta$ , the function  $g$  can be evaluated numerically.

Many distribution functions have analytical Laplace transforms. We discuss two of them: the constant and the gamma distributions.

(1) *Constant distribution*: The multirate mass transfer model reduces to a single rate model if the density function is temporally constant:

$$g = C_{im}^0 \beta e^{-\beta t} \quad (16a)$$

$$H = \beta^2 e^{-\beta t} \quad (16b)$$

(2) *Gamma distribution*: The gamma distribution is an important distribution in statistics. Its discussion and explanation can be found in many textbooks (e.g., [21]). The density function is given as

$$f(\beta) = \frac{b^a}{\Gamma(a)} \beta^{a-1} e^{-b\beta}, \quad a > 0, \quad b > 0 \quad (17)$$

For the mass transfer rate coefficient, its mean and variance are, respectively,

$$\langle \beta \rangle = a/b \quad \text{and} \quad \sigma^2 = a/b^2 \quad (18)$$

If the mean and variance are known, one can compute the values of  $a$  and  $b$  by

$$a = \langle \beta \rangle^2 / \sigma^2 \quad \text{and} \quad b = \langle \beta \rangle / \sigma^2 \quad (19)$$

The LT of a gamma distribution with parameters  $a$  and  $b$  is given as

$$\overline{f(s)} = (1 + s/b)^{-a} \quad (20)$$

After some algebraic manipulation, the functions  $g$  and  $H$  for gamma-distributed mass transfer rate coefficients are obtained as

$$g(t) = C_{im}^0 \langle \beta \rangle \left( \frac{b}{b+t} \right)^{a+1} \quad (21a)$$

$$H(t) = \sigma^2 (a+1) \left( \frac{b}{b+t} \right)^{a+2} \quad (21b)$$

Fig. 1 shows several examples of the gamma distribution of the mass transfer rate coefficient.

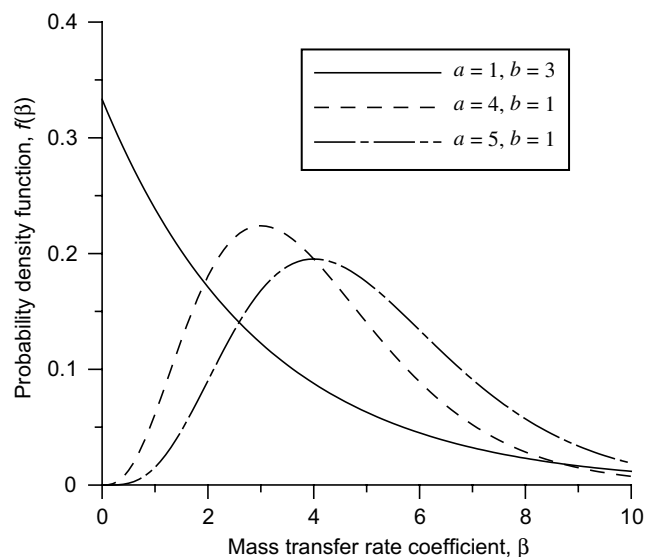


Fig. 1. Illustration of gamma distributions for the mass transfer rate coefficient.

### 3.2. Semi-analytical solution in Laplace space

As shown by Haggerty and Gorelick [12] and others, we can take the LT of (9) and obtain

$$s\overline{C_m} - C_m^0 = \overline{L(C_m)} - \phi\langle\beta\rangle\overline{C_m} + \phi\overline{g} + \phi\overline{HC_m} \quad (22)$$

Here we have relied on the LT properties of a derivative and convolution of two functions. Rearranging terms yields the concentration in Laplace-domain form

$$\overline{C_m} = \frac{\overline{L(C_m)} + C_m^0 + \phi\overline{g}}{s + \phi\langle\beta\rangle - \phi\overline{H}} \quad (23)$$

Inverting the LT generates a time-dependent solution for concentration in the mobile domain. The LT solution (23) is efficient and accurate, and particularly useful for analyzing forced-gradient tracer test data (e.g., [22,24]). However, because the LT solution converts the time domain into a new Laplace domain containing a new Laplace parameter, it is only applicable to transport in flow fields with constant velocities. In contrast, in our new approach, a LT form already exists in the IDE appearing in (5), and it is with respect to the mass transfer rate coefficient. After the transform is taken, the rate coefficient density function disappears and the LT is still in the time domain without introducing any new parameters. As a result, our new approach is applicable to transport in any spatially and temporarily varying velocity field.

### 3.3. Numerical solutions

For any realistic, complex aquifer, the solution to (5) can only be obtained by numerical techniques. Two such techniques are the finite-compartment approach previously described by Culver et al. [7] and the new direct integration approach developed in this study.

#### 3.3.1. Finite-compartment method

As shown by Culver et al. [7] and Cosler [6], a brute-force method can be used to solve the PDE given in (5) by truncating the infinite dimension of the distribution of the mass transfer rate coefficient into a finite number of values,  $k$ , each with a different constant rate coefficient. The integral is replaced by a summation:

$$\int_0^\infty f(\beta)\beta d\beta \approx \sum_{j=1}^k f_j\beta_j \quad (24)$$

where  $f_j$  is the percentage of the mass transfer rate coefficient  $\beta_j$  contained in bin  $j$ . The corresponding discretized PDEs become:

$$\frac{\partial C_m}{\partial t} = L(C_m) - \phi \sum_{j=1}^k f_j\beta_j(C_m - C_{im,j}) \quad (25a)$$

$$\frac{\partial C_{im}}{\partial t} = \beta_j(C_m - C_{im,j}), \quad j = 1, 2, \dots, k \quad (25b)$$

which can be solved implicitly or explicitly. An explicit scheme would be

$$C_m^{\text{new}} = C_m^{\text{old}} + \Delta t L(C_m^{\text{old}}) - \Delta t \phi \sum_{j=1}^k f_j\beta_j(C_m^{\text{old}} - C_{im,j}^{\text{old}}) \quad (26a)$$

$$C_{im,j}^{\text{new}} = C_{im,j}^{\text{old}} + \Delta t \beta_j(C_m^{\text{old}} - C_{im,j}^{\text{old}}) \quad j = 1, 2, \dots, k \quad (26b)$$

The advantage of this method is that it is simple and straightforward. The disadvantage is that it can be computationally inefficient if a large number of compartments,  $j$ , is required to represent the immobile domain when the mass transfer rate coefficient distribution has a large variance. Otherwise, the approach may result in large truncation errors.

#### 3.3.2. Direct integration method

To overcome the limitations of the finite-compartment method, we have developed a direct integration method as discussed next. The obstacle to evaluating the IDE in (9) is the convolution integral term  $\int_0^t H(t-\tau)C_m(\tau)d\tau$  because it involves the unknown solution and its historical trajectory since simulation time zero. Therefore, our method centers on the computation of the integral term. A simple, direct method is to save all the values of concentration and approximate the integral by a trapezoidal rule or Simpson's rule. When the simulation time is large, this method requires a considerable amount of computer memory. For small- or medium-sized transport models, however, this may not cause any problem.

It is straightforward to implement the direct integration method on a general advection–dispersion transport simulator such as MT3DMS [33] through an operator-splitting strategy. This can be accomplished by saving all concentration solutions at every time step since the beginning of the simulation period in computer memory or a disk file. A program module can be written to integrate these concentration solutions to obtain the value of the convolution integral term  $\int_0^t H(t-\tau)C_m(\tau)d\tau$  at the end of each advection–dispersion step. The concentration change due to the multirate mass transfer is then computed and added to those due to advection and dispersion. This procedure is repeated for the next time step until the end of the simulation period is reached.

When a transport model becomes large, to reduce computer memory requirements, the long historical concentration trajectory may have to be truncated. The next two schemes explore truncation of the integral in (9) using (1) direct truncation or (2) a finite Taylor series.

(1) *Direct integration with truncation:* For large time  $t$ , the integral can be truncated for the period prior to a time  $t_0$

$$\int_0^t H(t-\tau)C_m(\tau) d\tau \approx \int_{t_0}^t H(t-\tau)C_m(\tau) d\tau \approx \sum_{n=1}^{nt} \overline{H}_{nt-n} \overline{C}_m(\tau_n) \Delta t \quad (27)$$

where  $nt$  is the number of time steps from  $t_0$  to  $t$  and  $\overline{H}_n$  and  $\overline{C}_m(\tau_n)$  are the average values for the increment between  $n\Delta t$  and  $(n-1)\Delta t$ .

The value of  $nt$ , i.e., the number of terms required, depends on the integral function  $H$ . Fig. 2 shows the normalized function,  $H(t)/H(0)$ , for different values of mean and variance of mass transfer rate coefficient following a gamma distribution. The larger is the mean of the mass transfer rate coefficient, the faster the function value decreases with time. Except for the curve with a mean of 0.001 and a variance of  $1 \times 10^{-5}$ , all other curves show a rapidly decreasing trend. After  $t = 80$ , the value of the normalized function  $H(t)/H(0)$  has dropped to 1/100 of the initial value. Thus the number of truncation terms corresponding to  $t = 80$  might be considered appropriate for this particular example.

(2) *Finite Taylor series approximation:* Alternatively, we rewrite the function  $H$  as a Taylor series expanded at time  $t$

$$H(t-\tau) = H(t) + H'(t)(-\tau) + \frac{H''(t)}{2!}(-\tau)^2 + \dots = \sum_{k=0}^{\infty} \frac{H^{(k)}(t)}{k!}(-\tau)^k \quad (28)$$

After substituting (28) into the original convolution integral,  $\int_0^t H(t-\tau)C(\tau) d\tau$ , we obtain

$$\int_0^t H(t-\tau)C(\tau) d\tau = \sum_{k=0}^{\infty} \frac{H^{(k)}(t)(-1)^k}{k!} \int_0^t \tau^k C(\tau) d\tau = \sum_{k=0}^{\infty} \frac{H^{(k)}(t)(-1)^k}{k!} I_k(t) \quad (29)$$

where, in the last step, we have defined the integral by  $I_k(t) = \int_0^t \tau^k C(\tau) d\tau$ .

For numerical implementation, the infinite series is truncated at a large number of terms, say  $K$ , so  $\int_0^t H(t-\tau)C(\tau) d\tau$  becomes

$$\int_0^t H(t-\tau)C(\tau) d\tau \approx \sum_{k=0}^K \frac{H^{(k)}(t)(-1)^k}{k!} I_k(t) \quad (30)$$

Using this approach in a numerical model one needs to store  $K$  values of the integrals,  $I_k(t)$  for each active grid point. When the time advances from  $t$  to  $t + \Delta t$ , the integral can be updated as

$$I_k(t + \Delta t) = I_k(t) + \int_t^{t+\Delta t} \tau^k C(\tau) d\tau \quad (31)$$

The integral term can be simply approximated by

$$\int_t^{t+\Delta t} \tau^k C(\tau) d\tau \approx \frac{\Delta t}{2} [(t + \Delta t)^k C^{\text{new}} + t^k C^{\text{old}}] \quad (32)$$

where  $C(t) = C^{\text{old}}$  and  $C(t + \Delta t) = C^{\text{new}}$ .

If the concentration is approximated by a linear function on the interval  $(t, t + \Delta t)$ ,

$$C(\tau) = C^{\text{old}} + \frac{\Delta C}{\Delta t}(\tau - t), \quad t \leq \tau \leq t + \Delta t \quad (33)$$

where  $\Delta C = C^{\text{new}} - C^{\text{old}}$ , a more accurate approximation is simply

$$\int_t^{t+\Delta t} \tau^k C(\tau) d\tau \approx \frac{(t + \Delta t)^{k+1} C^{\text{new}} - t^{k+1} C^{\text{old}}}{k + 1} - \frac{\Delta C [(t + \Delta t)^{k+2} - t^{k+2}]}{\Delta t (k + 1)(k + 2)} \quad (34)$$

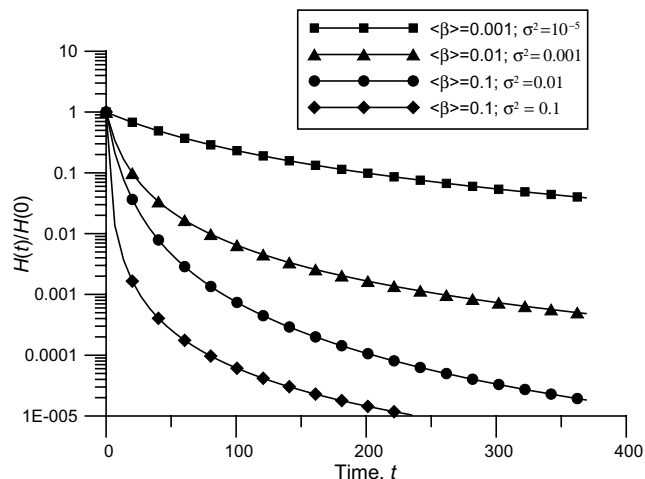


Fig. 2. An example of normalized function  $H(t)$  versus time  $t$ .

## 4. Numerical examples

### 4.1. Example 1: 1-D uniform flow field

The first example involves 1-D advective–dispersive transport in the mobile domain in a uniform semi-infinite flow field. The mass transfer between the mobile and immobile domains was governed by a multirate model with a gamma distribution for the first-order rate coefficient. A constant-concentration boundary condition was imposed at the origin. The concentration value at the constant-concentration source was equal to 1.0 for 200 days, and then zero for the remainder of the simulation period of 2000 days. Other flow and transport parameters for this example are listed in Table 1.

Table 1  
Flow and transport properties used in the two test examples

Parameter	Example 1	Example 2
Specific discharge, $q$ , (m/day)	0.06	(Variable)
Longitudinal dispersivity, $\alpha_L$ , (m)	10	10
Transverse dispersivity, $\alpha_T$ , (m)	$n/a$	1
Mobile domain porosity, $\theta_m$	0.2	0.24
Immobile domain porosity, $\theta_{im}$	0.05	0.06
Mean of the mass transfer rate coefficient, $\langle \beta \rangle$ , $d^{-1}$	$\frac{1}{50}$	$\frac{1}{60}$
Variance of the mass transfer rate coefficient, $\sigma^2$ , $d^{-2}$	0; $4 \times 10^{-3}$ and $4 \times 10^{-2}$	0 and $4 \times 10^{-3}$

Fig. 3 shows the concentration breakthrough curves in the mobile domain at an observation point located 200 m from the constant-concentration source using the direct integration method as given in (27) in comparison with the semi-analytic method of Haggerty and Reeves [14]. No truncation was involved in the numerical integration in this example and an accurate third-order TVD algorithm [33] was used to solve the advection–dispersion equation. The agreement between the two solution approaches is excellent with the root-mean-square (RMS) errors equal to  $1.55 \times 10^{-3}$ ,  $1.59 \times 10^{-3}$  and  $1.87 \times 10^{-3}$ , respectively, for the three variances of mass transfer rate coefficient of 0,  $4 \times 10^{-3}$  and  $4 \times 10^{-2}$ .

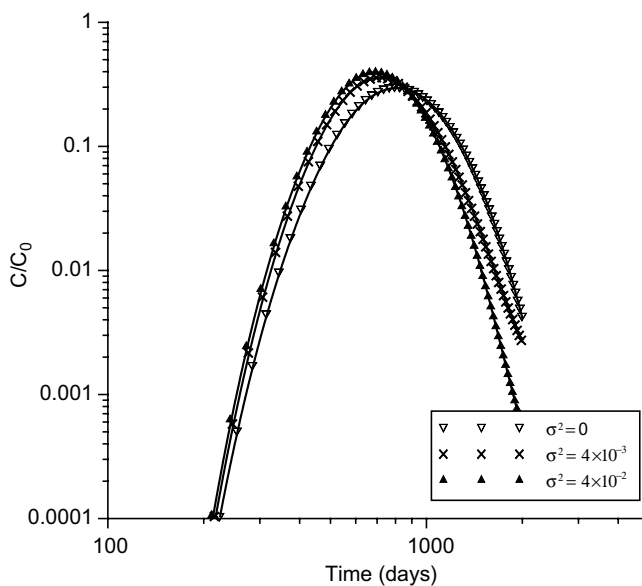


Fig. 3. Comparison of the multirate solutions for the 1D example. Symbols indicate the solutions obtained from this study and solid lines the semi-analytical solutions based on Haggerty and Reeves [14].

#### 4.2. Example 2: 2-D transient and random flow field

The second example involves advective–dispersive transport and multirate mass transfer in the flow field shown in Fig. 4a. The multirate mass transfer between the mobile and immobile domains is again governed by a gamma distribution for the first-order rate coefficient. We consider a confined aquifer that is 10m thick and under transient flow conditions. The flow domain is bounded by time-varying specified-head boundaries on the left and right borders and by no-flow boundaries on the upper and lower borders. For the transport model, the boundary conditions are zero-mass-flux on the left, upper and lower borders, and specified advective mass flux (zero concentration gradient) on the right border.

The hydraulic conductivity ( $K$ ) distribution used in the flow simulation is heterogeneous as illustrated in Fig. 4b. The random  $K$  distribution was generated by a random field generator assuming a  $\text{Ln}K$  mean and variance of 10 (m/day) and 1.0, respectively, and a correlation length of 100m. The simulation was divided into 10 stress periods of 36.5 days each with a total time of 365 days. The specified heads at the left and right boundaries were initially set to establish an ambient

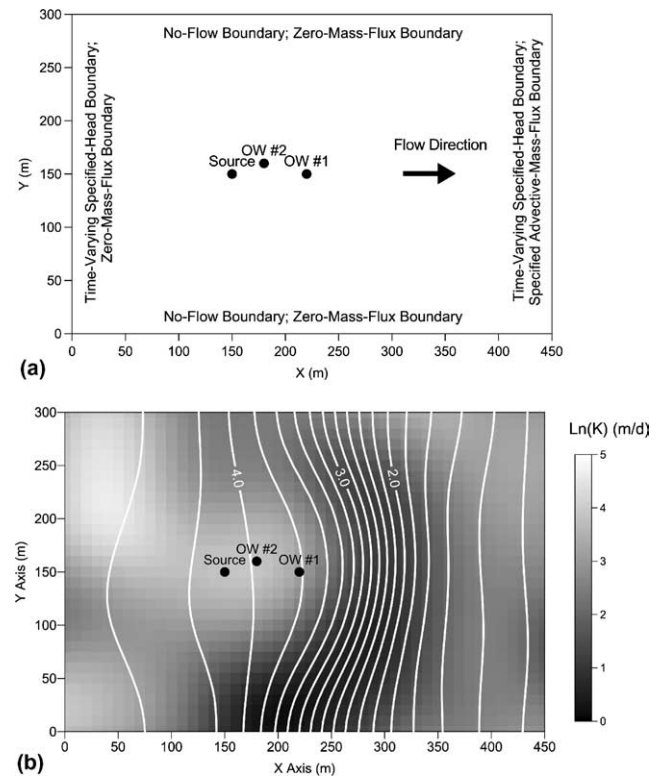


Fig. 4. Model setup for the 2-D test problem: (a) the boundary conditions for the flow and transport models and (b) hydraulic conductivity and resulting head distributions. Also shown are the locations of the contaminant source and two observation wells, OW #1 and OW #2.

hydraulic gradient of 0.01. The gradient decreased at a rate of  $2.22 \times 10^{-4}$  per stress period to induce a transient component. For simplicity, the storage coefficient for the confined aquifer was set to zero. Other flow and transport parameters for this example are listed in Table 1.

The aquifer was discretized into 46 columns and 31 rows with a regular spacing of 10 m in both directions. An initial relative concentration of 1.0 was assigned to a single cell (labeled 'Source' in Fig. 4a) to establish an instantaneous solute source near the left border. The first observation point, labeled 'OW #1', is located 70 m downstream from the source with the same  $y$  coordinate. The second observation point, labeled 'OW #2', is located 30 and 10 m from the source in the  $x$  and  $y$  axes, respectively. Fig. 4b shows the head solution at the end of the simulation period. The hydraulic gradient is larger where the hydraulic conductivity is smaller.

Fig. 5 shows the calculated breakthrough curves of relative concentrations in the mobile domain at the two observation points using the direct integration method as given in (27). When the variance of the gamma-distributed first-order mass transfer coefficient increases from zero (i.e., a single rate) to  $4 \times 10^{-3}$ , the calculated concentration is higher compared to that of the single-rate model at early times, but it becomes lower at later times. This is true at both observation points OW #1 and OW #2.

Under zero variance of the mass transfer rate coefficient, the multirate model is equivalent to a single-rate model. Fig. 6 shows the multirate solutions for zero variance obtained using the solution approach presented in

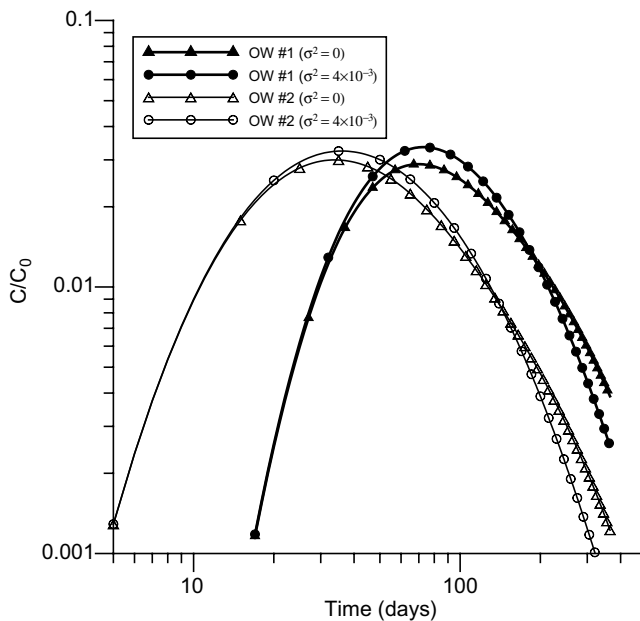


Fig. 5. Calculated breakthrough curves for the 2D example at two observation wells, OW #1 and OW #2 under two variances of the mass transfer rate coefficient.

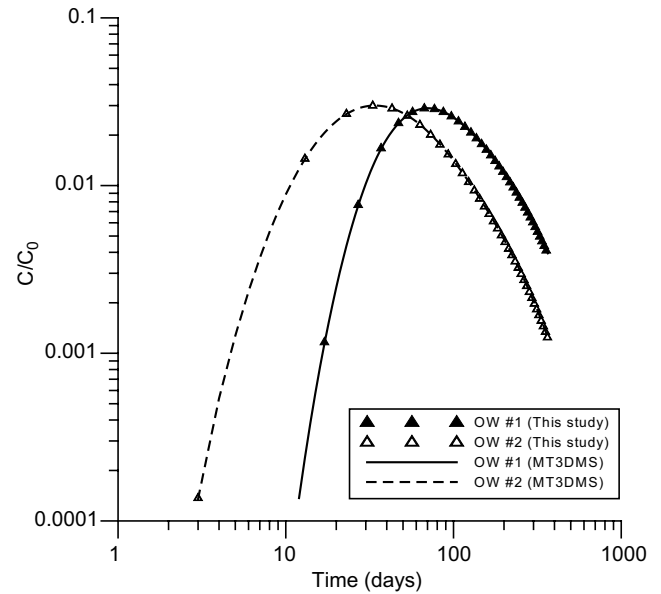


Fig. 6. Comparison of multirate solutions with zero variance of the mass transfer rate coefficient obtained from this study (symbols) and equivalent single-rate solutions obtained using the numerical simulator MT3DMS (solid lines).

this work and the single-rate solutions obtained using the numerical simulator MT3DMS [33]. The two sets of solutions are nearly identical, with the root-mean-square (RMS) errors equal to  $8.5 \times 10^{-5}$  and  $5.3 \times 10^{-5}$  for observation points OW #1 and OW #2, respectively.

For this test problem, all concentration values at different time steps were saved and used in the direction numerical integration to achieve the best accuracy for comparison with MT3DMS. The time step was set at 1 day for the case with zero variance of the mass transfer rate coefficient, and at 0.5 day for the case with a non-zero variance. Because the Peclet number was equal to 1 for this problem, the conventional finite-difference method was sufficiently accurate for solving the advection–dispersion part of the transport model.

To test how the truncation of the convolution integral function  $H$  (Eq. (29)) affects the accuracy of the multirate solution, we conducted a series of runs in which we started from a short integration length (more terms truncated) and progressively increased the integration length (fewer terms truncated). The RMS error of each obtained solution was compared with that of the exact solution without any truncation. Fig. 7 shows the results of the numerical experiment. For this 2-D test problem with a total simulation time of 365 days, it is apparent that the length of numerical integration longer than 80 days resulted in significantly diminished increases in the solution accuracy. In other words, the concentration solutions beyond the past 80 days may be safely truncated in the numerical integration of the past concentration history.

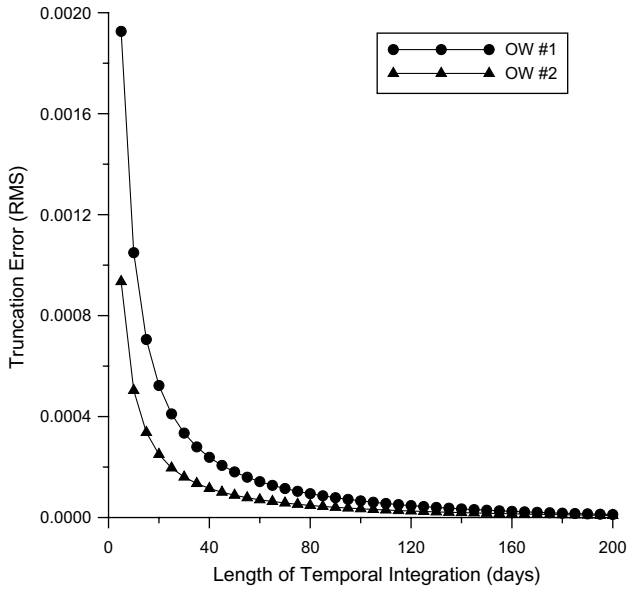


Fig. 7. Error in multirate solutions as a function of the truncated length of the concentration history.

## 5. Summary and discussion

We have presented a direct integration method that can be used to solve dual-domain multirate mass transfer coupled with advective–dispersive transport for systems that are not as restricted in complexity as those for which semi-analytic solutions exist. The basic strategy is to develop a single integral–differential equation for the concentration in the mobile domain. This was accomplished by separating the concentration in the immobile domain from the set of two partial differential equations. The method is general in the sense that it does not have any additional highly restrictive assumptions concerning the spatial and temporal variability of advection, dispersion, and sinks/sources in the mobile domain. In addition to the computation of advection, dispersion, and sinks/sources in the mobile domain, the new solution method requires the evaluation of a temporal integral of the concentration in the mobile domain. This concentration is a function of the Laplace transform of the distribution of the mass transfer rate coefficient.

We illustrated the approach for the case of gamma distribution functions for the mass transfer rate coefficient. Other distribution functions can also be implemented as long as the analytical Laplace transform exists. If not, the function  $H(t)$  can be approximated by a truncated Taylor's series involving higher moments of the mass transfer rate coefficient as shown in Appendix A. The direct integration method also allows the initial concentration in the immobile domain to be spatially varying dependent on the mass transfer coefficient, rather than being constant. The solutions for 1D and 2D examples obtained using the new approach

agree closely with those obtained by existing semi-analytical and numerical methods for the special circumstances under which those solutions exist.

The primary focus of this paper is to present a general solution approach to multirate mass transfer that mathematically requires neither rate compartmentalization nor temporal discretization. The approach we have developed can be used to obtain theoretically exact solutions as benchmarks for comparison with approximate solutions of multirate mass transfer under temporarily and spatially varying flow velocity distributions. This is an important contribution since it is the first time the exact solution has been presented along with a general means to obtain it. A detailed numerical analysis of our approach under realistic field conditions and various types of multirate distribution functions is beyond the scope of this paper and will be reported elsewhere in the future.

## Acknowledgments

This material is based upon work supported by the National Science Foundation under Grant Nos. EAR-0003511 and EAR-0003914. Any opinions, findings, and conclusions or recommendations expressed in this material are those of the author(s) and do not necessarily reflect the views of the National Science Foundation. The authors are grateful to Roy Haggerty of Oregon State University for providing us the *STAMMT-L* code used in this study, and to the four anonymous reviewers whose constructive comments have led to a significant improvement of the manuscript.

## Appendix A

Unlike the gamma distribution function, not every distribution function has a nice close-form LT. Examples of such functions are lognormal and heavy-tail distributions that are commonly used in practice. This appendix addresses what can be done if the close-form LT does not exist. If the distribution function does not have an analytic LT but its higher moments are available, functions  $g$  and  $H$  can be expressed in terms of those moments. Using Taylor series to expand the exponential term that appears in functions  $g(t)$  and  $H(t)$  we obtain

$$\begin{aligned}
 g(t) &= \int_0^\infty C_{\text{im}}^0 f(\beta) \beta e^{-\beta t} d\beta \\
 &= \int_0^\infty C_{\text{im}}^0 f(\beta) \beta \sum_{n=0}^\infty \frac{(-t\beta)^n}{n!} d\beta \\
 &= \sum_{n=0}^\infty \frac{(-t)^n}{n!} \langle C_{\text{im}}^0 \beta^{n+1} \rangle
 \end{aligned} \tag{A.1}$$

Again, when the initial concentration in the immobile domain is constant, we have

$$g(t) = C_{\text{im}}^0 \sum_{n=0}^{\infty} \frac{(-t)^n}{n!} \langle \beta^{n+1} \rangle \quad (\text{A.2})$$

Similarly we have

$$H(t) = \sum_{n=0}^{\infty} \frac{(-t)^n}{n!} \langle \beta^{n+2} \rangle \quad (\text{A.3})$$

To give an illustrative example, we know the lognormal distribution function does not have a close-form LT, but its moment is given as

$$\langle \beta^n \rangle = e^{n\mu + \frac{1}{2}n^2\sigma^2} \quad (\text{A.4})$$

## References

- [1] Barenblatt GE, Zheltov IP, Kochina IN. Basic concept of the theory of seepage of homogeneous liquids in fissured rocks. *J Appl Math Mech [English Trans]* 1960;24:1286–303.
- [2] Brusseau ML, Jessup RE, Rao PSC. Modeling the transport of solutes influenced by multiprocess nonequilibrium. *Water Resour Res* 1989;25(9):1971–88.
- [3] Brusseau ML, Gerstl Z, Augustijn D, Rao PSC. Simulating solute transport in an aggregated soil with the dual-porosity model: measured and optimized parameter values. *J Hydrol* 1994;163:187–93.
- [4] Coats KH, Smith BD. Dead-end pore volume and dispersion in porous media. *Soc Petrol Eng J* 1964(March):73–84.
- [5] Carrera J, Sánchez-Vila X, Benet I, Medina A, Galarza G, Guimerà J. On matrix diffusion: formulations, solution methods and qualitative effects. *Hydrogeol J* 1998;6(1):178–90.
- [6] Cosler DJ. Effects of rate-limited mass transfer on water sampling with partially-penetrating wells. *Ground Water* 2004;42(2):203–22.
- [7] Culver TB, Hallisey SP, Sahoo D, Deitsch JJ, Smith JA. Modeling the desorption of organic contaminants from long-term contaminated soil using distributed mass transfer rates. *Environ Sci Technol* 1997;31(6):1581–8.
- [8] Deans HA. A mathematical model for dispersion in the direction of flow in porous media. *Trans Soc Petrol Eng J* 1963:49–52.
- [9] Feehley CE, Zheng C, Molz FJ. A dual-domain mass transfer approach for modeling solute transport in heterogeneous porous media, application to the MADE site. *Water Resour Res* 2000;36(9):2501–15.
- [10] Gardner WR, Brooks RH. A descriptive theory of leaching. *Soil Sci* 1957;83:295–304.
- [11] Griffioen JW, Barry DA, Parlange JY. Interpretation of two-region model parameters. *Water Resour Res* 1998;34(3):373–84.
- [12] Haggerty R, Gorelick SM. Multiple-rate mass transfer for modeling diffusion and surface reactions in media with pore-scale heterogeneity. *Water Resour Res* 1995;31(10):2383–400.
- [13] Haggerty R, Gorelick SM. Modeling mass transfer processes in soil columns with pore-scale heterogeneity. *Soil Sci Soc Am J* 1998;62(1):62–74.
- [14] Haggerty R, Reeves PC. STAMMT-L 1.0, Formulation and User's Guide, Technical Report ERMS #520308, Sandia National Laboratories, Albuquerque, NM, 2002.
- [15] Haggerty R, Fleming SW, McKenna SA. STAMMT-R, Solute Transport and Multirate Mass Transfer in Radial Coordinates, Technical Report SAND 99-0164, Sandia National Laboratories, Albuquerque, NM, 1999.
- [16] Haggerty R, McKenna SA, Meigs LC. On the late-time behavior of tracer test breakthrough curves. *Water Resour Res* 2000;36(12):3467–80.
- [17] Haggerty R, Fleming SW, Meigs LC, McKenna SA. Tracer tests in a fractured 2. Analysis of mass transfer in single-well injection-withdrawal tests. *Water Resour Res* 2001;37(5):1129–42.
- [18] Haggerty R, Wondzell SM, Johnson MA. Power-law residence time distribution in the hyporheic zone of a 2nd-order mountain stream. *Geophys Res Lett* 2002;29(13). 10.1029/2002GL014743.
- [19] Harvey CF, Gorelick SM. Rate-limited mass transfer or macrodispersion: which dominates plume evolution at the Macrodispersion Experiment (MADE) site?. *Water Resour Res* 2000;36(3):637–50.
- [20] Herr M, Schafer G, Spitz K. Experimental studies of mass transport in porous media with local heterogeneities. *J Contaminant Hydrol* 1989;4(2):127–37.
- [21] Hogg RV, Craig AT. Introduction to mathematical statistics. 5th ed.. New Jersey: Prentice-Hall; 1995.
- [22] Hollenbeck KJ, Harvey CF, Haggerty R, Werth CJ. A method for estimating distribution of mass transfer rate coefficients with application to purging batch experiments. *J Contam Hydrol* 1999;37:367–88.
- [23] Julian HE, Boggs JM, Zheng C, Feehley CE. Numerical simulation of a natural gradient tracer experiment for the natural attenuation study: flow and physical transport. *Ground Water* 2001;39(4):534–45.
- [24] McKenna SA, Meigs LC, Haggerty R. Tracer tests in a fractured 3. Double-porosity, multi-rate mass transfer processes in convergent flow tracer tests. *Water Resour Res* 2001;37(5):1143–1154.
- [25] Rao PSC, Davidson JM, Jessup RE, Selim HM. Evaluation of conceptual models for describing non-equilibrium adsorption-desorption of pesticides during steady-flow in soils. *Soil Sci Soc Am J* 1979;43:22–8.
- [26] Rao PSC, Rolston DE, Jessup RE, Davidson JM. Solute transport in aggregated porous media: theoretical and experimental evaluation. *Soil Sci Soc Am J* 1980;44:1139–46.
- [27] Sardin M, Schweich D, Leij FJ, van Genuchten MT. Modeling the nonequilibrium transport of linearly interacting solutes in porous media, A review. *Water Resour Res* 1991;27(9):2287–307.
- [28] Skopp J, Warrick AW. A two-phase model for the miscible displacement of reactive solutes in soils. *Soil Sci Soc Am J* 1974;38:525–50.
- [29] Valocchi AJ. Use of temporal moment analysis to study reactive solute transport in aggregated porous media. *Geoderma* 1990;46:233–47.
- [30] van Genuchten MTh, Wierenga PJ. Mass transport studies in sorbing porous media. 2. Experimental evaluation with tritium ( $^3\text{H}_2\text{O}$ ). *Soil Sci Soc Am J* 1977;41:272–8.
- [31] Villermaux J. Chemical engineering approach to dynamic modeling of linear chromatography. A simple method for representing complex phenomena from simple concepts. *J Chromatogr* 1987;406:11–26.
- [32] Zhang Z, Brusseau ML. Nonideal transport of reactive solutes in heterogeneous porous. 5. Simulating regional-scale behavior of a trichloroethene plume during pump-and-treat remediation. *Water Resour Res* 1999;35(10):2921–35.
- [33] Zheng C, Wang PP. MT3DMS: A modular three-dimensional multispecies model for simulation of advection, dispersion and chemical reactions of contaminants in groundwater systems; Documentation and User's Guide Contract Report SERDP-99-1. U.S. Army Engineer Research and Development Center, Vicksburg, MS, 1999.
- [34] Zimmerman RW, Chen G, Hadgu T, Bodvarsson GS. A numerical dualporosity model with semianalytical treatment of fracture/matrix flow. *Water Resour Res* 1993;29(7):2127–37.